

CountTRuCoLa: Rule Confidence Learning for Temporal Knowledge Graph Forecasting

Julia Gastinger, Christian Meilicke, Heiner Stuckenschmidt

University of Mannheim
{first.last}@uni-mannheim.de

Abstract

We address the task of temporal knowledge graph (TKG) forecasting by introducing a fully explainable method based on temporal rules. Motivated by recent work proposing a strong baseline using recurrent facts, our approach learns four simple types of rules with a confidence function that considers both recency and frequency. Evaluated on nine datasets, our method matches or surpasses the performance of eight state-of-the-art models and two baselines, while providing fully interpretable predictions.

1 Introduction

Temporal knowledge graphs (TKG) extend static knowledge graphs with temporal information by using timestamps that indicate when a triple is valid (Han et al. 2021a). Their ability to represent evolving multi-relational data enables reasoning over changing knowledge in a variety of tasks, including temporal question answering (Saxena, Chakrabarti, and Talukdar 2021), knowledge graph completion (Cai et al. 2023), and fact validation (Soulard, Saïs, and Raad 2025). In recent years, the task of TKG forecasting, i.e. predicting future links in TKG, has attracted significant interest, leading to the development of diverse modeling approaches (Jin et al. 2020; Li, Sun, and Zhao 2022; Li et al. 2022) and domain-specific use cases in finance (Li et al. 2022), career trajectory prediction (Lee et al. 2025), and clinical prediction (Sun et al. 2025).

This paper is motivated by a recently introduced baseline for TKG forecasting (Gastinger et al. 2024b), which predicts future links purely based on the recurrence of facts. The authors demonstrate that despite its inability to capture complex dependencies, this baseline offers a competitive or even superior alternative to existing models on three out of five common datasets. These results challenge the capabilities of current models, which are often built on neural networks or use reinforcement learning architectures within a complex end-to-end architecture. Motivated by these considerations, we propose a deliberately simple and fully explainable method for TKG forecasting, which picks up some ideas from the baseline proposed in (Gastinger et al. 2024b) and extends it to a rule-based TKG forecasting model.

Our model comprises four types of rules, which cover simple frequency distributions of entities and relations as well as temporal regularities expressed as symbolic rules.

Each of these temporal rules is associated with a confidence function, which assigns a score to a prediction based on two features: the temporal distance to the most current relevant observation and the frequency of the occurrences of the relevant observation. Our temporal rules use only a single body atom, meaning that the prediction of a rule is caused by a single fact and its occurrence frequency.

Within this paper we present a comprehensive experimental study comparing our method to eight existing approaches and two baselines. The results of our experiments show that we outperform the other methods in terms of mean reciprocal rank on seven out of nine datasets. On one dataset the baseline mentioned above achieves the best scores. There is only one dataset where a complex model outperforms both the baseline and our rule-based approach. This is a surprising result, as it illustrates that a lightweight, interpretable model is not only competitive with, but even surpasses the predictive performance of existing models.

2 Related Work

Temporal knowledge graph forecasting has been addressed using a variety of approaches. Methods based on deep graph networks combine message-passing with sequential models to capture both structural and temporal patterns; notable examples include RE-Net (Jin et al. 2020), RE-GCN (Li et al. 2021b), xERTE (Han et al. 2021a), TANGO (Han et al. 2021b), RETIA (Liu et al. 2023a), and CEN (Li et al. 2022). Another line of work leverages reinforcement learning agents to discover temporal paths, such as CluSTeR (Li et al. 2021a) and TimeTraveler (Sun et al. 2021). Other approaches include history-based prediction in CyGNet (Zhu et al. 2021), the use of local and global encoders in TiRGN (Li, Sun, and Zhao 2022), contrastive learning in CENET (Xu et al. 2023), latent relation mining in L2TKG (Zhang et al. 2023), and temporal path encoding in TPAR (Chen et al. 2024). More recently, LLM-based models such as zrLLM (Ding et al. 2024) and GenTKG (Liao et al. 2024) have been proposed to incorporate semantic information into TKG forecasting.

In addition, rule-based approaches for TKG forecasting aim to learn interpretable temporal logic rules. TLogic learns rules via temporal random walks (Liu et al. 2022), while TRKG extends this by introducing acyclic and relaxed-time-constraint rules (Kiran, Maharana, and Polepalli 2023). TR-

Rules further extends TLogic by supporting acyclic rules and introducing a window confidence measure to address temporal redundancy (Li et al. 2023). TempValid (Huang et al. 2024) builds on TLogic rules but explicitly models temporal validity by treating confidence and decay coefficients as learnable parameters within a machine learning framework, applying an exponential decay transformation to temporal features and aggregating them linearly. While the implementation details are not fully specified, TempValid likely relies on a neural or similar differentiable model, which, together with advanced negative sampling strategies, improves predictive performance at the expense of interpretability. Further, several approaches combine rules with embedding-based methods—such as ALRE-IR (Mei et al. 2022), LogE-Net (Liu et al. 2023b), TECHS (Lin et al. 2023), and INFER (Li et al. 2025). These hybrid methods generally sacrifice interpretability due to their reliance on learned embeddings and neural components.

Lastly, two deterministic heuristic baselines have been introduced: EdgeBank (Poursafaei et al. 2022), developed for single-relational graphs, does not consider relation types or temporal differences and simply predicts the recurrence of the same subjects and objects. In contrast, the baseline named Recurrency Baseline (Gastinger et al. 2024b) predicts fact recurrence by incorporating the temporal distance and frequency of previous facts, and unlike EdgeBank, is relation-aware, modeling recurrence patterns separately for each relation type.

Positioning of our Work Among these, the works closest to ours are TLogic and TempValid. However, both approaches have a different language bias that allows them to learn rules of length greater than one, that is, rules with multiple atoms in the body. While this increases expressiveness, it also introduces noise and reduces interpretability. In contrast, our approach intentionally focuses on the simplest and most interpretable form: rules with a single body atom. However, we do not simply reduce complexity. Instead, we design these short rules to be richer and more nuanced. Specifically, we introduce additional rule types beyond those in TLogic and TempValid, namely rules with constants, and rules reflecting general distributions inherent in the dataset, thus supporting a broader set of temporal patterns. We also propose an improved temporal scoring function that learns parameters, enabling more accurate modeling of temporal dynamics. In this context, our method not only takes into account the time distance to the most recent occurrence of the rule body but, in contrast to TempValid and TLogic, also the frequency of occurrence. By simplifying the rule form while refining its predictive power, our method offers an interpretable and effective alternative for TKG forecasting. Finally, while our work is inspired by the Recurrency Baseline, it goes beyond simple recurrence by introducing additional rule types that learn dependencies across different relations and by employing a dedicated parametrized confidence function for each rule.

3 Background and Notation

A temporal knowledge graph (TKG) G is a set of quadruples (s, p, o, t) . We refer to $C(G) = \{s | (s, p, o, t) \in G\} \cup \{o | (s, p, o, t) \in G\}$ as entities (or constants) of G , $P(G) = \{p | (s, p, o, t) \in G\}$ as relations (or predicates) of G , $T(G) = \{t | (s, p, o, t) \in G\} \subset \mathbb{N}^+$ as timestamps of G . Timestamps may represent hours, days, years, or any other temporal granularity, depending on the dataset and use case. The semantic meaning of a quadruple (s, p, o, t) is that s is in relation p to o at time t . Thus, a quadruple can also be understood as a triple (s, p, o) that is additionally annotated with a timestamp t , which tells that the statement made by the triple is true at (or during) t .

Given a TKG G , TKG forecasting or extrapolation is the task of predicting quadruples (s, p, o, t^*) for future timestamps $t^* > \max(T(G))$ with $p \in P(G)$ and $s, o \in C(G)$. In this work we focus on the task of **entity forecasting**, that is, predicting object or subject entities for queries $(s, p, ?, t^*)$ or $(?, p, o, t^*)$. This task has become a common choice for measuring the predictive quality of TKG forecasting methods (Gastinger et al. 2023). Akin to static knowledge graph completion, TKG forecasting is approached as a ranking task (Han 2022). For a given query, which is usually derived from a quadruple in a test or validation set, a model needs to rank entities in $C(G)$ using a scoring function that assigns plausibility scores. Due to that specific setting, for each query, there is always a correct entity to predict.

To simplify the evaluation protocol, one can extend a TKG G by adding for each $(s, p, ?, t) \in G$ the inverse quadruple $(s, p^{-1}, ?, t)$ where $p^{-1} \notin P(G)$ denotes a fresh relation, which is used as inverse relation of p . This doubles the size of G and the number of relations. It allows to focus on object queries only by converting a subject query as $(?, p, o, t^*)$ into the equivalent object query $(o, p^{-1}, ?, t^*)$. We will see in the following section that it also reduces the number of required rules. Thus, we always extend a given TKG by its inverse quadruples. Note that most evaluation datasets are already available in that extended form.

We propose a model that learns logical rules to capture the temporal regularities inherent in G . In this context we use a prefix notation and understand relation p as a ternary predicate. We use a literal $p(s, o, t)$ as logical representation of a quadruple (s, p, o, t) . A logical rule is a disjunction of literals with at most one unnegated literal, for example, $l_0 \vee \neg l_1 \vee \dots \vee \neg l_n$. Rules are usually written in the equivalent implicative form $l_0 \leftarrow l_1 \wedge \dots \wedge l_n$. We call l_0 the head of the rule and $l_1 \wedge \dots \wedge l_n$ the body of the rule. Given a rule r , we use $h(r)$ to refer to its head and $b(r)$ to refer to its body.

Rules have already been applied successfully to static knowledge graph completion tasks (Rossi et al. 2021). The following rule might have been used in this context.

$$\text{workplace}(x, y) \leftarrow \text{livesIn}(x, y) \quad (1)$$

It says that someone who lives in a certain city, will also work in that city with a certain probability. In the non-temporal setting the confidence value of a rule determines (or is aggregated into) the plausibility score which defines the position of a candidate within a ranking for a given

query. The confidence of a rule r , which uses, for example, two variables x and y in its head and body, is defined, according to (Galárraga et al. 2013), as follows:

$$\text{conf}_r = \frac{|\{(c, d) \mid \theta_{x/c, y/d}(h(r) \wedge b(r)) \in G\}|}{|\{(c, d) \mid \theta_{x/c, y/d}(b(r)) \in G\}| + \mathcal{P}}$$

where $\theta_{x/c, y/d}$ denotes a substitution of the variables x and y by constants c and d from $C(G)$. Thus, the numerator counts all possible substitutions to replace variables x and y such that the resulting groundings of both head and body are true according to G . The denominator is the sum of counting the larger set of those groundings where the body only is true (the head might or might not be true) and a constant \mathcal{P} . If we ignore \mathcal{P} , the confidence value estimates the probability that r makes a correct prediction given G . \mathcal{P} , which is usually set to a small positive value, has been added to the denominator by (Meilicke et al. 2024) as a smoothing parameter that pushes the confidence score towards 0 if the number of groundings is low. While static knowledge graph completion works fine with static confidences, computing confidence values in the temporal case is less straightforward and requires to consider the distances between body and head groundings as input to confidence functions.

4 Approach

We explain how our approach finds and applies different rules, and how it learns temporal rule confidence functions such as shown in Figure 1, by counting occurrences of temporal triples. We refer to our approach as CountTRuCoLa (Temporal Rule Confidence Learning), or short rucola.

4.1 Rules

Our approach supports four types of rules. The most important type of rule, called xy -rule, is shown in (2).

$$h(x, y, t^*) \leftarrow b(x, y, t) \wedge t^* > t \quad (2)$$

Aside from the constraint $t^* > t$, which expresses that we make a prediction into the future t^* , xy -rules contain only a single logical body atom. We call xy -rules where $h = b$ recurrent xy -rules. These recurrent xy -rules correspond to the core element used in the baseline presented by (Gastinger et al. 2024b).

Rules (3) and (4) are examples for recurrent and non-recurrent xy -rules. Both rules might describe the regularities in the dating behavior of celebrities.

$$\text{dated}(x, y, t^*) \leftarrow \text{dated}(x, y, t) \wedge t^* > t \quad (3)$$

$$\text{engaged}(x, y, t^*) \leftarrow \text{dated}(x, y, t) \wedge t^* > t \quad (4)$$

Note that our approach does not support rules where the order of variables are flipped. We mentioned above that we extend each TKG by its inverse quadruples. For that reason a rule as $h(x, y, t^*) \leftarrow b(y, x, t)$ is equivalent to $h(x, y, t^*) \leftarrow b^{-1}(x, y, t)$.

In the following, we explain two things: first, how to use xy -rules to make a prediction; and second, what is required to determine the confidence score assigned to such a prediction. Suppose we are concerned with a query $h(c, ?, t^*)$.

Relevant xy -rules are those rules that use h in their head, for example, a rule $r = h(x, y, t^*) \leftarrow b(x, y, t) \wedge t^* > t$. Rule r predicts a candidate d , i.e., r predicts the quadruple $h(c, d, t^*)$, if there exists a $t' \in T(G)$ such that $b(c, d, t') \in G$. We can check this for a given d via a constant time lookup by using appropriate index structures and we can retrieve all predicted candidates in linear time with respect to the number of candidates.

For Temporal Knowledge Graphs, contrary to static KG, with respect to Rule 3, it makes a difference if x dated y two weeks ago, or two years ago. Moreover, it might also be important to know how often x and y have been on dates within a certain time span. Thus, the confidence function that we introduce later on makes use of all time stamps t' with $b(c, d, t') \in G$ to estimate the confidence of $h(c, d, t^*)$. More precisely, it uses the distances between all these time-stamps and t^* . We introduce $\Delta_{\theta_{x/c, y/d}}^{r, t^*}$ to refer to the set of these distances for the prediction $h(c, d, t^*)$ made by rule r :

$$\Delta_{\theta_{x/c, y/d}}^{r, G, t^*} = \{t^* - t' \mid \theta_{x/c, y/d, t/t'}(b(r)) \in G, t' \in T(G)\}$$

We use subscript $\theta_{x/c, y/d}$ to express that we are concerned with time distances for the prediction that we get if we substitute x by c and y by d in the body of r . This means that we need a single lookup to check if a rule fires and we need to retrieve $\Delta_{\theta_{x/c, y/d}}^{r, G, t^*}$ to compute how confident r is with respect to this prediction. This set of distances is used as input for the confidence function that we introduce in Section 4.2.

The second type of rule that we support, is a rule type that uses constants d and d' in head and body of the rule. We call an instance of the following rule type a c -rule.

$$h(x, d, t^*) \leftarrow b(x, d', t) \wedge t^* > t \quad (5)$$

The constants that appear in c -rules are usually frequent constants. The following example of a c -rule says that a person born in Amsterdam will (probably) study at the University of Amsterdam.

$$\text{studied}(x, uva, t^*) \leftarrow \text{born}(x, amsterdam, t) \wedge t^* > t \quad (6)$$

Similar to the xy -rule, a c -rule (5) predicts a candidate d , i.e., predicts the quadruple $h(c, d, t^*)$, if there exists $t' \in T(G)$ such that $b(c, d', t') \in G$. Compared to the xy -rule, the set of distances relevant for the confidence computation depends only on the x -substitution, which means that $\Delta_{\theta_{x/c}}^{r, G, t^*}$ is the relevant set given a c -rule r . The underlying mechanism requires a distinction between two directions. Please consult the Supplementary Material¹ for details.

We include two further types of rules that use a static confidence, similar to the confidence value shown in Section 3. These rules can also be understood as a means to capture very basic frequency distributions within the dataset. We call these rules z -rules (7) and f -rules (8).

$$p(x, d, t) \leftarrow \exists z p(x, z, t) \quad (7)$$

$$p(c, d, t) \leftarrow \exists z p(c, z, t) \quad (8)$$

¹<https://github.com/JuliaGast/counttrucola/blob/main/supplementarymaterial.pdf> for Supplementary Material.

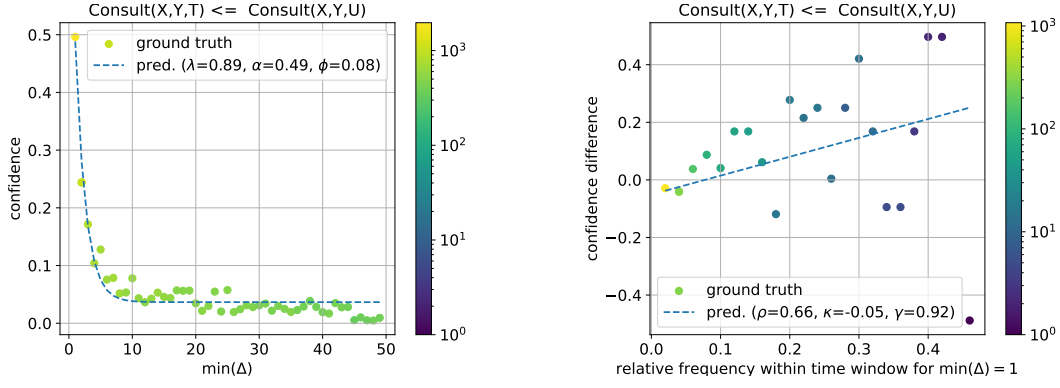


Figure 1: Examples E_r (points) and predicted curves (blue lines) for one rule r . Colors indicate the number of samples. Left: Learning f_r : Confidence as a function of $\min(\Delta)$. Right: Learning g_r : Residuals $\tilde{y} - f(\Delta)$ vs. frequency $\frac{|\Delta_{\mathcal{W}}|}{\mathcal{W}}$ for $\min(\Delta) = 1$.

Both rules types, contrary to xy -rules and c -rules use the same timestamp t in the head and in the body. Due to the evaluation protocol explained above, if we are asked a query $p(s, ?, t^*)$, we are justified to assume that there exists a correct answer, i.e. that we can assume $\exists z p(s, z, t^*)$, which corresponds to the body of a z -rule and a f -rule.

The following two examples illustrate the difference between these rule types.

$$\text{eats}(x, \text{pizza}, t) \leftarrow \exists z \text{ eats}(x, z, t) \quad (9)$$

$$\text{eats}(\text{kim}, \text{pizza}, t) \leftarrow \exists z \text{ eats}(\text{kim}, z, t) \quad (10)$$

The confidence value of (9) corresponds to the probability that someone eats pizza, if that person eats something. The confidence value of (10) corresponds to the probability that Kim eats pizza, if she eats something. Depending on Kim's eating habits, these numbers might diverge significantly. We compute the confidences for z and f -rules following the definition in Section 3. However, we count not only over constants but over combinations of constants and timestamps.

Finally, we have to clarify that xy -rules and c -rules have also an additional existentially quantified atom similar to the body atom of the z -rule and f -rule, namely the atom $\exists z h(x, z, t^*)$. If we are asked a query $h(s, ?, t^*)$ we are justified to assume that this atom is true due to the fact that the query is asked. Remember that each query has always at least one correct answer. Thus, the additional atom makes no difference when answering a query, but makes a difference when collecting the examples to learn the confidence function from.

We construct each possible xy -rule ($|P(G)|^2$ combinations), each z -rule ($|P(G)| \times |C(G)|$ combinations) and each f -rule ($|P(G)| \times |C(G)|^2$ combinations). These numbers are an upper bound. The actual numbers are much lower, as certain combinations of constants and relations do not appear together. However, the combinatorial space is too large for mining all c -rules. For that reason we collect a subset of all c -rules that make use of the most frequent constants only.

4.2 Temporal Confidence Functions

Each xy - and c -rule is associated with a parameterized temporal confidence function. In this section, we introduce a

three-step procedure for learning these functions, and conclude with an illustrative example. Note that all steps rely exclusively on information from the training set.

Collecting Examples We explain in the following, given a rule r , how to collect the examples E_r required to learn the parameters of r . We introduce a notation $G^t = \{(s, p, o, t') \mid (s, p, o, t') \in G \wedge t' < t\}$ that allows us to refer to the subset of G that contains all quadruples up to a certain timestamp t .

Algorithm 1: Collecting Examples

```

1: Input: TKG  $G$ ,  $xy$ -rule  $r = h(x, y, t^*) \leftarrow b(x, y, t)$ 
2: Output: examples set  $E_r$ 
3:  $E_r = \emptyset$ 
4: for  $t \in T(G)$  do
5:   for  $c, d \in C(G)$  do
6:     if  $\exists z h(c, z, t) \in G$  then
7:        $\Delta = \Delta_{\theta_{x/c, y/d}^{r, G^t, t}}$ 
8:       if  $h(c, d, t) \in G$  then add  $(\Delta, 1)$  to  $E_r$ 
9:       else add  $(\Delta, 0)$  to  $E_r$ 

```

The procedure for collecting the examples for an xy -rule $r = h(x, y, t^*) \leftarrow b(x, y, t)$ is shown in Algorithm 1. The outer loop iterates over all timestamps in $T(G)$, while the inner loop iterates over all pairs (c, d) with $c, d \in C(G)$. For each combination it checks if there exists some z with $h(c, z, t) \in G$ to ensure that only those examples, which appear in an evaluation query, are considered. Then we collect the time distances from the $\theta_{x/c, y/d}$ -substitution if applied to r for making a prediction at timestamp t . If the prediction is correct, we store the set of distances as a positive example, if the prediction is incorrect, we store it as negative example. Actually, in Line 7, we only collect distances within a time window \mathcal{W} , where \mathcal{W} is a hyperparameter.

For a c -rule, the procedure is the same with two minor modifications. We can omit to loop over d and, as there is no variable y in the rule body, we have to drop y/d from the substitution $\theta_{x/c, y/d}$.

Confidence Function To compute the confidence of a xy or c -rule with respect to the time differences between body

and head, we use $\Delta_{\theta_{x/c,y/d}}^{r,G,t^*}$, which we denote by Δ for simplicity. Our confidence function for a rule r is defined by:

$$\text{conf}_r(\Delta) = f_r(\Delta) + g_r(\Delta) \quad (11)$$

The first summand, f_r , describes the effect of the most recent occurrence, i.e., the smallest time distance $\min(\Delta)$, of the body grounding:

$$f_r(\Delta) = \alpha_r \cdot \frac{1}{1 + \phi_r} \cdot (2^{-\lambda_r \cdot (\min(\Delta) - 1)} + \phi_r) \quad (12)$$

where $\alpha_r, \lambda_r, \phi_r \in \mathbb{R}_0^+$ are learnable parameters.

The second summand, g_r , captures the effect of the frequency, i.e., the number of occurrences $|\Delta|$, of the body grounding:

$$g_r(\Delta) = \min(\max(\rho_r \frac{|\Delta_{\mathcal{W}}|}{\mathcal{W}} + \frac{\kappa_r}{\min(\Delta)}, -\gamma_r), \gamma_r) \quad (13)$$

where $\Delta_{\mathcal{W}}$ denotes the set of body groundings whose time difference is at most \mathcal{W} , i.e., $\Delta_{\mathcal{W}} = \{d \in \Delta : d \leq w\}$, with \mathcal{W} being a hyperparameter. Further, $\rho_r, \kappa_r, \gamma_r \in \mathbb{R}$ are learnable parameters. Note that the additive offset in g_r depends inversely on $\min(\Delta)$. Intuitively, when $\min(\Delta)$ is low, a high proportion of the window \mathcal{W} can contain body groundings. In contrast, when $\min(\Delta)$ is high, the maximum possible number of additional groundings in $\Delta_{\mathcal{W}}$ is reduced, since the upper limit for $|\Delta_{\mathcal{W}}|$ becomes $w - \min(\Delta) + 1$.

Each parameter in the confidence function has a specific and interpretable role:

- α : scales the f_r score and determines its value when $\min(\Delta) = 1$.
- λ : specifies the decay rate, determining how quickly f_r decreases as $\min(\Delta)$ increases. When $\lambda = 0$, the time distance between body and head has no effect while higher values result in faster decay.
- ϕ : determines the asymptotic lower bound of f_r as $\min(\Delta) \rightarrow \infty$.
- ρ : defines the slope of the frequency term g_r . When $\rho = 0$, frequency has no impact; for larger ρ , the score increases proportionally with observed frequency.
- κ : acts as an additive offset modulated by $\min(\Delta)$.
- γ : bounds the frequency score via clipping, ensuring that the overall impact of g_r remains within $[-\gamma, \gamma]$.

Learning the Confidence Functions Our approach learns a confidence function for each rule by optimizing the parameters $(\alpha_r, \lambda_r, \phi_r, \rho_r, \kappa_r, \gamma_r)$ aiming to minimize the sum of squared errors between the predicted confidence $\text{conf}_r(\Delta)$ (Equation 11) and the observed confidence values from the examples E_r . Recall that E_r for a rule r consists of N examples (Δ_i, y_i) , where $i = 1, \dots, N$. Here, y_i is the truth value indicating whether a body and head grounding appeared together (1) or not (0). For simplicity, we omit the subscript r in the following.

Following the approach of (Meilicke et al. 2024) for confidence computation in static KGs (see Section 4), we adjust the observed confidence values by adding a constant \mathcal{P} to

the denominator. Here, \mathcal{P} is a hyperparameter. Unlike the static setting, we apply this transformation separately for each $\min(\Delta)$. We denote this transformation as s , yielding the modified observed confidence value $\tilde{y}_i = s(\Delta_i, y_i)$. Details of this computation are provided in Algorithm A.1 in the supplementary material.

To learn the confidence function, we conduct two steps:

Step 1. We estimate α, λ, ϕ by minimizing the sum of squared errors (SSE) between the predictions of f and the transformed observed confidence values \tilde{y} , assuming the contribution of g is zero:

$$\arg \min_{\alpha, \lambda, \phi} \sum_{(\Delta_i, y_i) \in E} (f(\Delta_i) - s(\Delta_i, y_i))^2. \quad (14)$$

Step 2. Next, we estimate ρ, κ, γ , fixing the parameters of f obtained in Step 1. We minimize the SSE between $f + g$ and the transformed observed confidence values:

$$\arg \min_{\rho, \kappa, \gamma} \sum_{(\Delta_i, y_i) \in E} (f(\Delta_i) + g(\Delta_i) - s(\Delta_i, y_i))^2. \quad (15)$$

This two-step approach represents a practical compromise. While it does not guarantee a globally optimal solution, in practice it significantly reduces training time without noticeably impacting prediction accuracy.

Table 1: An example for a test query and rules. We use c for relation *Consult*, and e for *Express_intent_to_cooperate*.

| Query: <i>Consult</i> (<i>Hollande</i> , ?, 351), Ground Truth: <i>Merkel</i> CountTRuCoLa Prediction: <i>Merkel</i> , Score: 0.68 | | | | |
|--|-------------|--|--------------------|--|
| conf_r | $f_r + g_r$ | rule | $ \min(\Delta_r) $ | $\frac{ \Delta_r _{\mathcal{W}}}{\mathcal{W}}$ |
| 0.41 | 0.44-0.03 | $c(x, y, t^*) \leftarrow e^{-1}(x, y, t)$ | 1 | 2/50 |
| 0.40 | 0.43-0.03 | $c(x, y, t^*) \leftarrow e(x, y, t)$ | 1 | 2/50 |
| 0.17 | | $c(\text{Holl.}, \text{Merkel}, t) \leftarrow \exists z c(\text{Holl.}, z, t)$ | | |
| 0.13 | 0.10+0.03 | $c(x, y, t^*) \leftarrow c(x, y, t)$ | 4 | 3/50 |
| 0.13 | 0.10+0.03 | $c(x, y, t^*) \leftarrow c^{-1}(x, y, t)$ | 4 | 3/50 |

Illustration by Example Figure 1 illustrates the learned confidence functions and the example set E_r for a representative rule r for ICEWS14. Figure 1 (left) plots the learned $f(\Delta)$ (in blue) and the confidence values (points), where the color indicates the number of examples for each $\min(\Delta)$. The predicted confidence decreases with increasing $\min(\Delta)$, following the exponential decay pattern. This is consistently observed across many rules and datasets. Figure 1 (right) plots the learned $g(\Delta)$ for $\min(\Delta) = 1$ (blue) and difference between the confidence values and the prediction from f , i.e. $\tilde{y} - f(\Delta)$ (points). For clarity, we present only the case where $\min(\Delta) = 1$. The figure shows that for the given rule, higher frequency of the rule body correlates with higher confidence scores.

Table 1 shows an example test query, along with CountTRuCoLa’s highest-scoring prediction and its score. It also displays the rules that contribute to this prediction score

(among them the rule from Figure 1), their individual component scores, the distance to the most recent occurrence, and the frequency of occurrences within the window \mathcal{W} .

Overall, examples like this help uncover not just *why* certain predictions are made, but also surface model and dataset characteristics. These are valuable both for model trust and further refinement.

4.3 Aggregation

As illustrated in Table 1, if our approach predicts a candidate c , it is typically predicted by several rules r_0, \dots, r_n with different confidence scores s_0, \dots, s_n . For instance, the candidate *Merkel* is predicted by five rules with scores 0.41, ..., 0.13. Combining these confidence scores is known as rule aggregation problem (Betz et al. 2024).

A common strategy for rule aggregation is the *noisy-or* strategy, which computes $1 - \prod_{i=0}^n (1 - s_i)$. Because noisy-or assumes independence among rules, we adopt the version proposed by (Betz et al. 2024) that applies noisy-or to the top \mathcal{H} confidences (e.g., $\mathcal{H} = 5$). We treat \mathcal{H} as a hyperparameter. Additionally, we introduce a decay factor $\mathcal{D} \in [0, 1]$ as hyperparameter. Let s_1, \dots, s_n be sorted in descending order; we apply a modified noisy-or where each s_i is replaced by $s_i \cdot \mathcal{D}^i$, giving less weight to lower-ranked scores. The Supplementary Material summarizes all hyperparameters.

5 Experiments

5.1 Experimental Setup

For our experiments, we use the **datasets** from TGB 2.0 *smallpedia*, *polecat*, *icews*, *wikidata* (Gastinger et al. 2024a), and the datasets *ICEWS14/18*, *GDELT*, *YAGO*, *WIKI*, in the versions as used in (Gastinger et al. 2023; Li et al. 2021b)².

We follow the **evaluation protocol** from (Gastinger et al. 2023), and use the TGB 2.0 evaluation framework (Gastinger et al. 2024a). We report time-aware filtered mean reciprocal rank (MRR) and Hits@10. All experiments are conducted for single-step prediction.

We **compare our model to 8 methods** of the 23 methods described in Section 2, as well as the two heuristic baselines EdgeBank and the Recurrency Baseline (Rec.B). Unless otherwise stated, we report results for these 10 methods based on the evaluations in (Gastinger et al. 2024a) (for the TGB 2.0 datasets) and (Gastinger et al. 2023) (for all other datasets). For TiRGN, we report the results from the original papers and perform a sanity check of the released code. We exclude 15 prior methods from direct comparison for reasons such as incompatible evaluation protocols, unavailable code, or differences in datasets; detailed justifications are provided in the supplementary material.

All experiments run on a SLURM-managed CPU cluster running the AlmaLinux 9.5 operating system. Nodes featured Intel Xeon (E5-2640 v2/v3/v4, Silver 4114) and AMD EPYC (7413, 7713P, 9474F) processors, with up to 96 cores and 1.5 TB RAM per node. We did not use GPUs.

²More information on the datasets including a table with dataset statistics can be found in the supplementary material.

Please find the code to reproduce our experiments on GitHub³.

5.2 Results

Table 2 reports test scores on all nine datasets. CountTRuCoLa achieves the highest test MRR on seven datasets and the second highest on the remaining two, demonstrating strong overall predictive performance. While the Hits@10 performance is slightly lower (best on five of nine), this is likely because hyperparameter tuning was performed based on validation MRR. On one dataset the Recurrency Baseline achieves the best scores. There is only one dataset where a complex model outperforms both the baseline and our approach. CountTRuCoLa also achieves considerable improvements compared to the Recurrency Baseline on *ICEWS14*, *smallpedia*, and *polecat*. This highlights that rules, which capture more than recurrency, along with learning confidence functions, leads to better performance.

Notably, unlike other methods that fail due to out-of-time (OOT) or out-of-memory (OOM) issues on large-scale graphs, CountTRuCoLa scales to all datasets without such failures. The results illustrate that a lightweight, interpretable model is not only competitive with, but even surpasses the predictive performance of existing models while maintaining scalability.

A note on GDELT We observe that CountTRuCoLa underperforms the Recurrency Baseline on *GDELT*, despite outperforming all other models. *GDELT*, based on a platform that sources global news events, features extremely fine-grained temporal resolution of 15 minutes. This often leads to repeated mentions of the same event across adjacent timestamps due to media redundancy, e.g., the triple (*IRAN*, *Criticize_or_denounce*, *PAKISTAN*) appearing eight times within 31 hours. In summary, we find two temporal patterns: (i) short-term repetition driven by media coverage, and (ii) long-term dependencies, such as a country criticizing another in response to a military action. The gap between CountTRuCoLa and the baseline is likely due to its difficulty in disentangling the two types of temporal patterns.

Ablation Studies Table 3 shows ablation studies on *ICEWS14* and *WIKI*. First, we analyze the contributions of different rule types, see part (a) of Table 3. For *ICEWS14*, *xy*-rules yield the highest MRR, which is expected since they form the core of our approach. Combining the individual rule types (row *all*) leads to the highest scores. However, the MRR scores do not simply add up due to overlapping predictions among rule types. We further evaluate the importance of each rule type by removing them individually. The removal leads to a performance decrease, with the most substantial drop observed when *xy*-rules are excluded. This highlights the benefit of incorporating multiple rule types.

For *WIKI*, the ablation study reveals a different behavior. Here, using only the recurrency rules already achieves the same results as combining all rule types. This suggests two things: First, only very simple dependencies need to be captured to achieve strong predictive performance on this

³ <https://github.com/JuliaGast/counttrucola>

Table 2: Comparison of models on nine benchmark datasets. An entry OOM means Out Of Memory (40 GB GPU or 1056 GB RAM), an entry OOT means Out Of Time (7 days), an entry - means, no results have been reported on this dataset.

| | GDEL T | | YAGO | | WIKI | | ICEWS14 | | ICEWS18 | | smallp. | | polecat | | icews | | wikidata | |
|------------------------------|-------------|-------------|-------------|-------------|-------------|-------------|-------------|-------------|-------------|-------------|-------------|-------------|-------------|-------------|-------------|-------------|-------------|-------------|
| | MRR | H10 | MRR | H10 | MRR | H10 | MRR | H10 | MRR | H10 | MRR | H10 | MRR | H@10 | MRR | H10 | MRR | H10 |
| TRKG | 21.5 | 37.3 | 71.5 | 79.2 | 73.4 | 76.2 | 27.3 | 50.8 | 16.7 | 35.4 | - | - | - | - | - | - | - | - |
| xERTE | 18.9 | 32.0 | 87.3 | 91.2 | 74.5 | 80.1 | 40.9 | 57.1 | 29.2 | 46.3 | - | - | - | - | - | - | - | - |
| TANGO | 19.2 | 32.8 | 62.4 | 67.8 | 50.1 | 52.8 | 36.8 | 55.1 | 28.4 | 46.3 | - | - | - | - | - | - | - | - |
| Timetraveler | 20.2 | 31.2 | 87.7 | 91.2 | 78.7 | 83.1 | 40.8 | 57.6 | 29.1 | 43.9 | - | - | - | - | - | - | - | - |
| TiRGN | 21.7 | 37.6 | 88.0 | 92.9 | 81.7 | 87.1 | 44.0 | 63.8 | 33.7 | 54.2 | - | - | - | - | - | - | - | - |
| TLogic | 19.8 | 35.6 | 76.5 | 79.2 | 82.3 | 87.0 | 42.5 | 60.3 | 29.6 | 48.1 | 59.5 | 70.7 | 22.8 | 37.8 | 18.6 | 30.1 | OOT | OOT |
| RE-GCN | 19.8 | 33.9 | 82.2 | 88.5 | 78.7 | 84.7 | 42.1 | 62.7 | 32.6 | 52.6 | 59.4 | 68.7 | 17.5 | 29.2 | 18.2 | 33.1 | OOM | OOM |
| CEN | 20.4 | 35.0 | 82.7 | 89.4 | 79.3 | 84.9 | 41.8 | 60.9 | 31.5 | 50.7 | 61.2 | 70.5 | 18.4 | 32.3 | 18.7 | 33.4 | OOM | OOM |
| EdgeBank _{tw} | 1.9 | 3.5 | 61.7 | 61.7 | 58.5 | 84.4 | 13.5 | 34.2 | 7.2 | 17.9 | 35.3 | 56.6 | 5.6 | 11.9 | 2.0 | 5.8 | 53.5 | 59.6 |
| Rec.B ($\psi_{\Delta\xi}$) | 24.5 | 39.8 | 90.9 | 93.0 | 81.4 | 87.1 | 37.4 | 51.5 | 28.7 | 43.6 | 60.5 | 71.6 | 19.8 | 31.7 | 21.1 | 32.4 | OOT | OOT |
| Rucola | 23.8 | 40.3 | 90.9 | 93.2 | 82.7 | 86.6 | 45.0 | 62.0 | 32.8 | 51.0 | 64.4 | 71.7 | 25.6 | 40.8 | 21.4 | 32.1 | 60.9 | 62.8 |

Table 3: Ablation study. Test scores for all rule types as introduced in Section 3, and for different scoring functions.

| | | WIKI | | ICEWS14 | |
|---------------------|-----------------------------------|------|------|---------|------|
| | | MRR | H10 | MRR | H10 |
| (a) Rule Types | rec-rules | 82.6 | 86.3 | 35.6 | 47.3 |
| | xy -rules (incl. rec.) | 82.5 | 86.3 | 42.8 | 60.4 |
| | c -rules | 29.6 | 30.0 | 25.2 | 34.6 |
| | z -rules | 14.1 | 24.9 | 14.1 | 27.9 |
| | f -rules | 67.5 | 82.8 | 34.0 | 46.5 |
| | all - z -rules | 82.6 | 86.4 | 44.7 | 61.6 |
| | all - f -rules | 82.6 | 86.5 | 43.5 | 61.3 |
| | all - c -rules | 82.6 | 86.5 | 44.8 | 61.7 |
| | all - (xy -rules (incl. rec.)) | 68.5 | 83.2 | 39.0 | 53.1 |
| | all | 82.6 | 86.6 | 45.0 | 62.0 |
| (b) Conf. Functions | static | 68.0 | 82.7 | 39.9 | 58.5 |
| | g_r | 68.6 | 83.2 | 43.4 | 59.5 |
| | f_r | 81.1 | 86.5 | 44.7 | 61.8 |
| | $f_r + g_r$ | 82.6 | 86.6 | 45.0 | 62.0 |

dataset; and second, CountTRuCoLa is robust against potential noise introduced by additional rules.

Second, we analyze the benefit of our introduced scoring functions, see part (b) of Table 3, comparing four variants: (i) a static confidence; (ii) using only f (Equation 12), setting the output of g to zero, i.e., predicting based on the most recent body grounding; (iii) using only g (Equation 13) setting the output of f to zero, i.e., predicting based on the frequency of the body grounding; (iv) the default CountTRuCoLa setting combining f and g (Equation 11). For both datasets combining the two scores into a single confidence function that accounts for both recency and frequency leads to considerable improvements over the other options. Each component on its own also improves predictive performance compared to static confidence. In addition, incorporating the frequency of body groundings improves predictive capability compared to relying solely on recency.

6 Discussion

Within this paper we propose a rule-based approach for TKG forecasting. The rules supported by our approach are extremely simple. Each rule is triggered by a single triple and its occurrences scattered over different timestamps (xy and c -rules), or reflects a general distribution inherent in the dataset (f and z -rules). Moreover, we do not learn a complex weighting scheme but use a canonical aggregation model, which is a modified variant of the well known noisy-or model. As a consequence, our approach is fully interpretable. Its outcomes are easy to understand. Each prediction can be traced back to the regularity and the specific observation that resulted in this prediction.

Our approach outperforms current state-of-the-art on most datasets. This might be a surprising result, as we do not propose a complex end-to-end architecture, but an approach that is limited in its expressivity. Our findings raise an important question: Are complex architectures really necessary and beneficial for TKG forecasting? The superior performance of our simple rule-based approach suggests that, at least for existing datasets, much of what is gained from complexity is in fact explainable by simple dependencies. Complex end-to-end architectures are **not** required to achieve competitive predictive results on the standard evaluation datasets. Their inability to outperform our simpler method on standard datasets may reflect an absence of truly complex temporal patterns, difficulties distinguishing them from noise, or limitations in current model designs.

While our approach outperforms or matches more sophisticated methods in average test scores, we cannot claim that such models would not excel on queries where truly complex temporal patterns exist. A thorough interpretability analysis of these models, possibly on a per-query basis, was beyond the scope of this work. However, such analyses could help clarify whether those models capture meaningful patterns missed by our method.

Taking a step back to focus on simplicity and transparency for TKG forecasting has proven valuable, paving the way for future work to build on these findings and to rethink existing assumptions about model design in TKG forecasting.

References

- Betz, P.; Lüdtkke, S.; Meilicke, C.; and Stuckenschmidt, H. 2024. Rule confidence aggregation for knowledge graph completion. In *International Joint Conference on Rules and Reasoning*, 32–49. Springer.
- Cai, B.; Xiang, Y.; Gao, L.; Zhang, H.; Li, Y.; and Li, J. 2023. Temporal Knowledge Graph Completion: A Survey. In *Proceedings of the Thirty-Second International Joint Conference on Artificial Intelligence, IJCAI*.
- Chen, K.; Wang, Y.; Li, Y.; Li, A.; Yu, H.; and Song, X. 2024. A Unified Temporal Knowledge Graph Reasoning Model Towards Interpolation and Extrapolation. In *Proceedings of the 62nd Annual Meeting of the Association for Computational Linguistics (ACL) (Volume 1: Long Papers)*.
- Ding, Z.; Cai, H.; Wu, J.; Ma, Y.; Liao, R.; Xiong, B.; and Tresp, V. 2024. zrLLM: Zero-Shot Relational Learning on Temporal Knowledge Graphs with Large Language Models. In *Proceedings of the 2024 Conference of the North American Chapter of the Association for Computational Linguistics: Human Language Technologies (Volume 1: Long Papers)*, 1877–1895.
- Galárraga, L. A.; Teflioudi, C.; Hose, K.; and Suchanek, F. 2013. AMIE: association rule mining under incomplete evidence in ontological knowledge bases. In *Proceedings of the 22nd international conference on World Wide Web*, 413–422.
- Gastinger, J.; Huang, S.; Galkin, M.; Loghmani, E.; Parviz, A.; Poursafaei, F.; Danovitch, J.; Rossi, E.; Koutis, I.; Stuckenschmidt, H.; Rabbany, R.; and Rabusseau, G. 2024a. TGB 2.0: A Benchmark for Learning on Temporal Knowledge Graphs and Heterogeneous Graphs. In *38th Conference on Neural Information Processing Systems (NeurIPS), Datasets and Benchmarks Track*.
- Gastinger, J.; Meilicke, C.; Errica, F.; Szttyler, T.; Schuelke, A.; and Stuckenschmidt, H. 2024b. History repeats itself: A Baseline for Temporal Knowledge Graph Forecasting. In *Proceedings of the Thirty-Third International Joint Conference on Artificial Intelligence, IJCAI 2024, Jeju, South Korea*.
- Gastinger, J.; Szttyler, T.; Sharma, L.; Schuelke, A.; and Stuckenschmidt, H. 2023. Comparing Apples and Oranges? On the Evaluation of Methods for Temporal Knowledge Graph Forecasting. In *Joint European Conference on Machine Learning and Knowledge Discovery in Databases (ECML PKDD)*, 533–549.
- Han, Z. 2022. *Relational learning on temporal knowledge graphs*. Phd thesis, Ludwig-Maximilians-University, Munich, Germany.
- Han, Z.; Chen, P.; Ma, Y.; and Tresp, V. 2021a. Explainable Subgraph Reasoning for Forecasting on Temporal Knowledge Graphs. In *9th International Conference on Learning Representations (ICLR)*.
- Han, Z.; Ding, Z.; Ma, Y.; Gu, Y.; and Tresp, V. 2021b. Learning Neural Ordinary Equations for Forecasting Future Links on Temporal Knowledge Graphs. In *Proceedings of the 2021 Conference on Empirical Methods in Natural Language Processing (EMNLP)*, 8352–8364.
- Huang, R.; Wei, W.; Qu, X.; Zhang, S.; Chen, D.; and Cheng, Y. 2024. Confidence is not timeless: Modeling temporal validity for rule-based temporal knowledge graph forecasting. In *Proceedings of the 62nd Annual Meeting of the Association for Computational Linguistics (Volume 1: Long Papers)*, 10783–10794.
- Jin, W.; Qu, M.; Jin, X.; and Ren, X. 2020. Recurrent Event Network: Autoregressive Structure Inference over Temporal Knowledge Graphs. In *Proceedings of the 2020 Conference on Empirical Methods in Natural Language Processing (EMNLP)*, 6669–6683.
- Kiran, R. U.; Maharana, A.; and Polepalli, K. R. 2023. A Novel Explainable Link Forecasting Framework for Temporal Knowledge Graphs Using Time-Relaxed Cyclic and Acyclic Rules. In *Proceedings of the 27th Pacific-Asia Conference on Knowledge Discovery and Data Mining (PAKDD), Part I*, 264–275.
- Lee, Y.-C.; Lee, J.; Yamashita, M.; Lee, D.; and Kim, S.-W. 2025. CAPER: Enhancing Career Trajectory Prediction using Temporal Knowledge Graph and Ternary Relationship. In *Proceedings of the 31st ACM SIGKDD Conference on Knowledge Discovery and Data Mining V.1, KDD '25*. New York, NY, USA: Association for Computing Machinery. ISBN 9798400712456.
- Li, N.; E, H.; Li, S.; Sun, M.; Yao, T.; Song, M.; Wang, Y.; and Luo, H. 2023. TR-Rules: Rule-based Model for Link Forecasting on Temporal Knowledge Graph Considering Temporal Redundancy. In Bouamor, H.; Pino, J.; and Bali, K., eds., *Findings of the Association for Computational Linguistics (EMNLP)*, 7885–7894. Singapore: Association for Computational Linguistics.
- Li, N.; Haihong, E.; Yao, T.; Hu, T.; Li, Y.; Luo, H.; Song, M.; and Zhu, Y. 2025. INFER: A Neural-symbolic Model For Extrapolation Reasoning on Temporal Knowledge Graph. In *The Thirteenth International Conference on Learning Representations*.
- Li, Y.; Sun, S.; and Zhao, J. 2022. TiRGN: Time-Guided Recurrent Graph Network with Local-Global Historical Patterns for Temporal Knowledge Graph Reasoning. In *Proceedings of the 31st International Joint Conference on Artificial Intelligence (IJCAI)*, 2152–2158.
- Li, Z.; Guan, S.; Jin, X.; Peng, W.; Lyu, Y.; Zhu, Y.; Bai, L.; Li, W.; Guo, J.; and Cheng, X. 2022. Complex Evolutional Pattern Learning for Temporal Knowledge Graph Reasoning. In *Proceedings of the 60th Annual Meeting of the Association for Computational Linguistics (ACL), Volume 2: Short Papers*, 290–296.
- Li, Z.; Jin, X.; Guan, S.; Li, W.; Guo, J.; Wang, Y.; and Cheng, X. 2021a. Search from History and Reason for Future: Two-stage Reasoning on Temporal Knowledge Graphs. In *Proceedings of the 59th Annual Meeting of the Association for Computational Linguistics and the 11th International Joint Conference on Natural Language Processing (ACL/IJCNLP), Volume 1: Long Papers*, 4732–4743.
- Li, Z.; Jin, X.; Li, W.; Guan, S.; Guo, J.; Shen, H.; Wang, Y.; and Cheng, X. 2021b. Temporal Knowledge Graph Reasoning Based on Evolutional Representation Learning. In *The*

44th International ACM SIGIR Conference on Research and Development in Information Retrieval (SIGIR).

Liao, R.; Jia, X.; Li, Y.; Ma, Y.; and Tresp, V. 2024. GenTKG: Generative Forecasting on Temporal Knowledge Graph with Large Language Models. In *Findings of the Association for Computational Linguistics: NAACL 2024*, 4303–4317.

Lin, Q.; Liu, J.; Mao, R.; Xu, F.; and Cambria, E. 2023. TECHS: Temporal Logical Graph Networks for Explainable Extrapolation Reasoning. In *Proceedings of the 61st Annual Meeting of the Association for Computational Linguistics (ACL), Volume 1: Long Papers*, 1281–1293.

Liu, K.; Zhao, F.; Xu, G.; Wang, X.; and Jin, H. 2023a. RETIA: Relation-Entity Twin-Interact Aggregation for Temporal Knowledge Graph Extrapolation. In *39th IEEE International Conference on Data Engineering (ICDE)*, 1761–1774.

Liu, Y.; Ma, Y.; Hildebrandt, M.; Joblin, M.; and Tresp, V. 2022. TLogic: Temporal Logical Rules for Explainable Link Forecasting on Temporal Knowledge Graphs. In *36th Conference on Artificial Intelligence (AAAI)*, 4120–4127.

Liu, Y.; Mo, Y.; Chen, Z.; and Liu, H. 2023b. LogE-Net: Logic Evolution Network for Temporal Knowledge Graph Forecasting. In *International Conference on Artificial Neural Networks (ICANN)*, 472–485.

Mei, X.; Yang, L.; Cai, X.; and Jiang, Z. 2022. An Adaptive Logical Rule Embedding Model for Inductive Reasoning over Temporal Knowledge Graphs. In *Proceedings of the 2022 Conference on Empirical Methods in Natural Language Processing (EMNLP)*, 7304–7316.

Meilicke, C.; Chekol, M. W.; Betz, P.; Fink, M.; and Stuckeschmidt, H. 2024. Anytime bottom-up rule learning for large-scale knowledge graph completion. *The VLDB Journal*, 33(1): 131–161.

Poursafaei, F.; Huang, S.; Pelrine, K.; and Rabbany, R. 2022. Towards Better Evaluation for Dynamic Link Prediction. In *36th Conference on Neural Information Processing Systems (NeurIPS), Datasets and Benchmarks Track*, 32928–32941.

Rossi, A.; Barbosa, D.; Firmani, D.; Matinata, A.; and Meri- aldo, P. 2021. Knowledge graph embedding for link prediction: A comparative analysis. *ACM Transactions on Knowledge Discovery from Data (TKDD)*, 15(2): 1–49.

Saxena, A.; Chakrabarti, S.; and Talukdar, P. P. 2021. Question Answering Over Temporal Knowledge Graphs. In *Proceedings of the 59th Annual Meeting of the Association for Computational Linguistics and the 11th International Joint Conference on Natural Language Processing, ACL/IJCNLP, (Volume 1: Long Papers)*, 6663–6676. Association for Computational Linguistics.

Soulard, T.; Saïs, F.; and Raad, J. 2025. Explainable Temporal Fact Validation Through Constraints Discovery in Knowledge Graphs. In *The Semantic Web - 22nd European Semantic Web Conference, ESWC 2025, Proceedings, Part I*, volume 15718 of *Lecture Notes in Computer Science*, 227–244. Springer.

Sun, H.; Zhong, J.; Ma, Y.; Han, Z.; and He, K. 2021. Time-Traveler: Reinforcement Learning for Temporal Knowledge

Graph Forecasting. In *Proceedings of the 2021 Conference on Empirical Methods in Natural Language Processing (EMNLP)*, 8306–8319.

Sun, Z.; Qu, X.; Yang, Y.; Song, C.; Li, D.; Jiang, Z.; and Zhang, R. 2025. Temporal Knowledge Graph Reasoning with Reinforcement Learning for Clinical Gastritis Prediction. In *Proceedings of the 2024 10th International Conference on Communication and Information Processing, ICCIP '24*. New York, NY, USA: Association for Computing Machinery. ISBN 9798400717444.

Xu, Y.; Ou, J.; Xu, H.; and Fu, L. 2023. Temporal Knowledge Graph Reasoning with Historical Contrastive Learning. In *37th Conference on Artificial Intelligence (AAAI)*, 4765–4773.

Zhang, M.; Xia, Y.; Liu, Q.; Wu, S.; and Wang, L. 2023. Learning Latent Relations for Temporal Knowledge Graph Reasoning. In *Proceedings of the 61st Annual Meeting of the Association for Computational Linguistics (ACL), Volume 1: Long Papers*, 12617–12631.

Zhu, C.; Chen, M.; Fan, C.; Cheng, G.; and Zhang, Y. 2021. Learning from History: Modeling Temporal Knowledge Graphs with Sequential Copy-Generation Networks. In *35th Conference on Artificial Intelligence (AAAI)*, 4732–4740.